IEEE Photonics Journal
An IEEE Photonics Society Publication

Open Access

Intrinsically Stabilized Plastic Optical Fiber Link Subject to External Optical Feedback

Volume 11, Number 01, February 2019

Azusa Inoue, *Member, IEEE*
Yasuhiro Koike, *Member, IEEE*

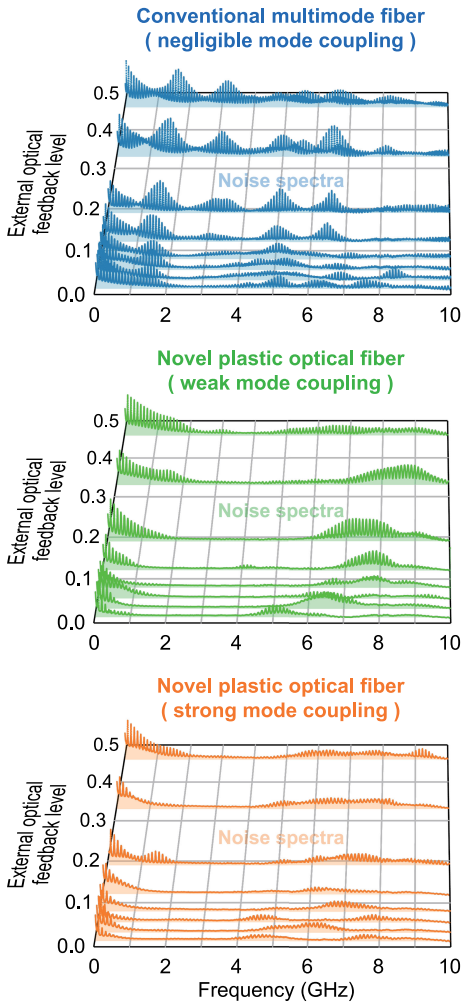

DOI: 10.1109/JPHOT.2019.2891703

IEEE photonics SOCIETY

IEEE

Intrinsically Stabilized Plastic Optical Fiber Link Subject to External Optical Feedback

Azusa Inoue, *Member, IEEE*, and Yasuhiro Koike, *Member, IEEE*

Graduate School of Science and Technology, Keio Photonics Research Institute, Keio University, Kawasaki 212-0032, Japan

DOI:10.1109/JPHOT.2019.2891703

Manuscript received December 6, 2018; revised December 25, 2018; accepted January 5, 2019. Date of publication January 9, 2019; date of current version February 11, 2019. Corresponding authors: Azusa Inoue and Yasuhiro Koike (e-mail: inoue@kpri.keio.ac.jp; koike@appi.keio.ac.jp).

Abstract: We develop a graded-index plastic optical fiber (GI POF) that can significantly stabilize a multimode fiber (MMF) link with a vertical-cavity surface-emitting laser (VCSEL) subject to external optical feedback. It is demonstrated that the dominant mechanism for this stabilization effect is the strong mode coupling of the GI POF, which is closely related to the polymer-specific microscopic heterogeneities in the GI POF core material. Such mode coupling decreases correlation between the problematic reflected light field and VCSEL cavity field, increasing tolerance of the MMF link for external optical feedback. Our developed GI POF with specific microscopic heterogeneities prevents the external-optical-feedback-induced critical destabilization observed for silica GI MMFs. These results suggest that the stabilization effect can be controlled by microscopic properties regardless of the fiber attenuations and core refractive indices.

Index Terms: Optical interconnects, waveguides, scattering.

1. Introduction

Internet traffic continues to grow with an increase in the network connections of smartphones, tablets, televisions, and various monitoring devices as we approach the Internet-of-Things (IoT) era. This growth is being accelerated by the implementation of ultrahigh-definition (UHD) imaging technologies into IoT environments. To accommodate this traffic, core/metro/access networks including datacenter networks have been rapidly developed. For distribution and acquisition of UHD video data through existing networks, UHD videos are highly compressed. However, UHD device connections require decompressed data transmission with a bit rate well above 100 Gb/s for video formats with 8K (7680 $\times$ 4320) resolution. Nevertheless, optical fibers have not been introduced into homes and buildings located in the optical network terminal area where UHD devices are used.

In UHD applications, short optical cables are frequently connected and disconnected in a manner similar to metal interface cables. Under such conditions, data transmission stabilities are significantly degraded by various noises that are not problematic for commonly used 2-level pulse amplitude modulation (PAM) in conventional optical links. This degradation becomes pronounced for multilevel modulation schemes such as 4-level PAM (PAM-4) that are vital for data transmission at more than 100 Gb/s [1], [2].

Graded-index plastic optical fibers (GI POFs) are promising for indoor applications because of their flexibility, safety, and high bandwidth [3], [4], which enables 40-Gb/s data transmission through a single 100-m GI POF. Recently, we proposed a low-noise GI POF to achieve stable and robust data transmission in a multimode fiber (MMF) link with a vertical-cavity surface-emitting laser (VCSEL) [5]. The low-noise GI POF has microscopic heterogeneities in the core material that can induce random mode coupling through polymer-specific light scattering. The strong mode coupling observed in the GI POF can significantly decrease noise and instability including those due to external optical feedback; however, the detailed mechanisms underlying this stabilization have not yet been clarified. The significant link stabilization suggested that any interferometric noise (e.g., multipath interference [6], modal noise [7], and polarization noise [8]) could be decreased through the mode coupling in the low-noise GI POF. Here, we demonstrate that a GI POF can prevent critical destabilization in a VCSEL-based MMF link subject to external optical feedback. We show that the dominant mechanism for this stabilization effect is strong mode coupling, which is closely related to the microscopic heterogeneities in the polymer core material. This suggests that the stabilization effect can be controlled by the microscopic core material properties regardless of the fiber attenuations and core refractive indices. Such link stabilization using the optical fiber itself will facilitate highly stable multilevel transmission in VCSEL-based MMF links for the upcoming IoT era.

2. Mode Coupling in GI POF

Using the co-extrusion method [3], we fabricated low-noise GI POF X and Y with different mode coupling strengths. Both fibers had core diameters of $\sim$50 μm and numerical apertures (NAs) of $\sim$0.2. The measured attenuations of GI POF X and Y were 0.04 dB/m and 0.06 dB/m, respectively. Under power-law approximations of the GI profiles, the GI POFs had refractive index profiles with an index exponent of $\sim$2.0, which is comparable to a design index-exponent for a reference silica GI MMF with the same core diameter and NA as the GI POFs. We evaluated the 1-m GI POFs because the attenuations and dispersions in the short fibers barely influenced 10-Gb/s data transmission qualities. Both fibers had bandwidths well above the device limit of 26.5 GHz, which were measured by a component analyzer.

The only source of random mode coupling in a silica MMF is microbending [9]. Generally, mode coupling in a silica GI MMF is pronounced for fiber lengths of the order of hundreds of meters. However, the GI POFs have stronger mode couplings, which can be observed even for a fiber length of 1 m; this reflects their different coupling mechanism, which is closely related to microscopic heterogeneities with large-scale density and composition fluctuations in the core polymers [10], [11]. Recently, we have developed a coupled power equation for mode coupling due to these microscopic heterogeneities, which cannot be analyzed by the original theory under the assumption of directional perturbations along fiber axes (e.g., microbending) [12]. For the low-noise GI POFs, power coupling coefficients or coupling strengths of propagation mode pairs can be approximately expressed by

$$h_{ij} \approx \langle \delta \varepsilon_r^2 \rangle \frac{\varepsilon_0^2 \omega^2 \pi^{3/2} a^3}{8} \int\int \left| \boldsymbol{E}_i^* \cdot \boldsymbol{E}_j \right|^2 \mathrm{d}x\mathrm{d}y, \tag{1}$$

where $\boldsymbol{E}_{i(j)}$ is the transverse electric field vector for mode $i(j)$, ω is the angular frequency of the guided light, and ε_0 is the vacuum dielectric constant. As shown in (1), mode coupling strength depends on correlation length a and the mean square $\langle \delta \varepsilon_r^2 \rangle$ in the relative dielectric constant fluctuations of the microscopic heterogeneities that do not exist in silica glasses. The polymers consist of extremely large polymer coils with sizes on the order of hundreds of angstroms, resulting in density and composition fluctuations at different scales. Microscopic heterogeneities have been confirmed from the light scattering patterns of the polymer bulks [3]; it is difficult to directly observe and evaluate microscopic heterogeneities in the actual GI POF core. In this study, using our coupled power theory for analyses of the frequency response of the GI POFs [11], average coupling coefficients of GI POF X and Y for all guided mode pairs were estimated to be 7.6×10^{-5} m^{-1} and 1.0×10^{-3} m^{-1}, respectively. These values correspond to relative dielectric constant fluctuations on the order of 10^{-7} and correlation lengths on the order of several hundreds of nanometers.

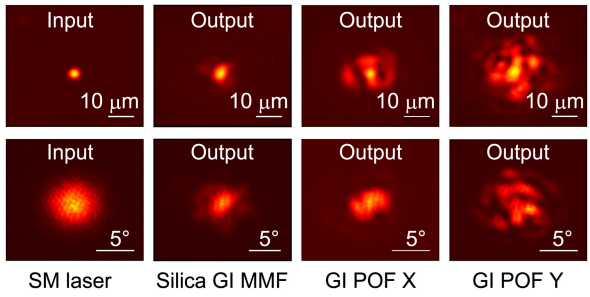

Fig. 1. NFPs (top) and FFPs (bottom) of input laser beam, output beam from a silica GI MMF, output beam from GI POF X, and output beam from GI POF Y under center launching conditions with an SMF-pigtailed single longitudinal mode laser.

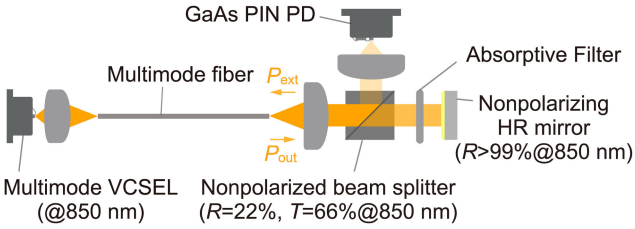

Fig. 2. External optical feedback level is defined by $R_{ext} = P_{ext}/P_{out}$, where P_{out} and P_{ext} are powers of the output beam from a fiber and the re-entered beam to a fiber, respectively.

Fig. 1 shows near-field patterns (NFPs) and far-field patterns (FFPs) of output beams from the silica GI MMF and low-noise GI POFs. The launching condition was center launching using a single longitudinal mode laser pigtailed with a polarization-maintaining single-mode fiber (SMF), which has an angled physical contact connector, a mode field diameter (MFD) of ~5.3 μm, and a laser linewidth of 10 MHz. The silica GI MMF had NFP and FFP that well correlated with those of the launched mode. In contrast, the NFP and FFP of the low-noise GI POF significantly differed from the silica GI MMF, being more pronounced for GI POF Y with its stronger mode coupling. The beam pattern changes of the low-noise GI POFs could be attributed to random power transition from the launched modes to the other guided modes through the mode coupling. This mode coupling effect can significantly decrease the influence of any external optical feedback from the back of the fiber because fractions of the back-reflected lights self-coupled to the VCSEL cavity are decreased through decorrelation of their field patterns with VCSEL modes. In actual optical modules for MMF links, the optical feedback from a fiber input face tends to barely influence system stability owing to sufficiently short external-cavity length, whose round-trip frequency is much higher than typical VCSEL relaxation frequencies [13], [14].

3. Optical-Feedback-Insensitive GI POF Link

Fig. 2 shows the experimental setup. The VCSEL was directly modulated with 10-Gb/s non-return-to-zero (NRZ) data (a 2^{31}–1 pseudorandom bit-sequence pattern length) at a bias current of 5 mA, where the bandwidth was ~9 GHz and the average relaxation frequency was ~6 GHz. The VCSEL modulation voltage was 0.07 V, which was less than or comparable to a minimum symbol-level difference of a PAM-4 with the VCSEL, and was much lower than the typical voltages of 0.35–0.4 V for NRZ (PAM-2) with the VCSEL. The GaAs PIN photodiode (PD) had a bandwidth of ~12 GHz. We measured the bit error rate (BER) for the 10-Gb/s data transmission in the MMF links with the low-noise GI POFs and silica GI MMF subject to external optical feedback from the back of the fiber. Output beams from the fibers were collimated and divided with a nonpolarized beam splitter (BS). Reflected light from the BS was focused and detected by the PD. Transmitted lights through the BS

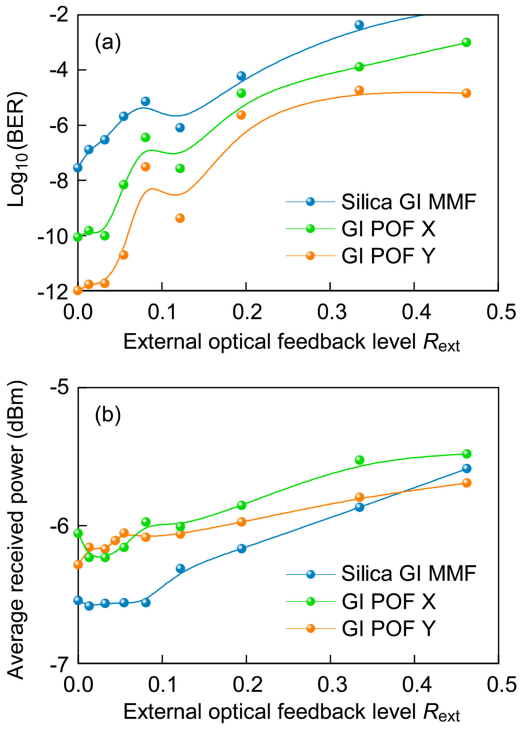

Fig. 3. (a) BERs and (b) average received powers for silica GI MMF, GI POF X, and GI POF Y as functions of external optical feedback level. All BERs were measured for 10 min, which was sufficiently long to achieve a confidence level above 99% for BERs below 10^{-12} by the measurement without bit errors. To remove the influence of the initial transient response, the BER measurement began 1 min after the modulation signal was injected into the VCSEL.

were back-reflected on a high-reflection (HR) mirror to the MMF links as external optical feedback whose level was controlled using an antireflection (AR)-coated absorptive filter between the BS and HR mirror, as shown in Fig. 2. All lenses were AR-coated. Insertion loss of the BS in the MMF link was ~6.6 dB, which corresponds to the sum of the absorption, scattering, and transmittance of the BS.

As shown in Fig. 3(a), the BERs for all fibers tended to increase with an increase in the level of external optical feedback from the HR mirror. However, the BERs were significantly decreased by simply replacing the silica GI MMF with the low-noise GI POF for all feedback levels. This BER improvement was more pronounced for GI POF Y with its stronger mode coupling. Moreover, GI POF Y had almost the same BERs despite increase in the back-reflected light power for feedback levels above ~0.2. These results suggest that the low-noise GI POF can prevent critical destabilization observed for the silica GI MMF. Fig. 3(b) shows the corresponding average powers received with the PD for the silica GI MMF and low-noise GI POFs as functions of the external optical feedback level. In the MMF link without optical feedback from the HR mirror ($R_{ext} = 0$), the received power for the low-noise GI POFs were higher than the silica GI MMF. This was mainly due to the lower refractive indices of the fiber core or lower Fresnel loss at the fiber facets, as compared with the silica GI MMF. For all fibers, the received power tended to increase with an increase in external optical feedback level. However, the low-noise GI POF decreased the feedback-induced increase in received power, being more pronounced for the stronger mode coupling of GI POF Y. This feature also suggests the stabilization effects of the low-noise GI POF.

In the setup shown in Fig. 2, the VCSEL stability is influenced by both optical feedback from the fiber output face and the HR mirror. Therefore, the level of net optical feedback, R_{net}, that influences the VCSEL stability is approximately expressed by

$$R_{net} = \eta_c(1 - A_f)^2(1 - R_f)^2[R_f + (1 - R_f)^2 R_{ext}]. \quad (2)$$

Here, we ignored the interference of the back-reflected lights from the reflectors and multiple reflections between the reflectors for simplicity. In (2), the first and second terms on the right-hand side correspond to the optical feedback from the fiber output facet and HR mirror, respectively. R_f is the fiber facet reflectivity and A_f is the fiber attenuation, which corresponds to $-10\log(1-A_f)$ in units of dB; η_c is the fraction of back-reflected light self-coupled in a VCSEL cavity. This coupling fraction depends on back-reflected light characteristics such as field pattern, degree of polarization, and degree of coherence [15], which change through light scattering or random mode coupling in the low-noise GI POF.

As shown in (2), the net optical feedback level depends on R_f or the core refractive index. The dependence of R_{net} on R_f changes with increasing R_{ext} values, and the signs of the derivative $\partial R_{net}/\partial R_f$ change from positive to negative at R_{ext}, given by $(1-3R_f)/4(1-R_f)^2$, which has almost the same values around 0.24 for most optical fiber core refractive indices from 1.35 to 1.60 [3]. Therefore, a lower core refractive index results in a lower R_{net} for R_{ext} below $\sim$0.24 and a higher R_{net} for R_{ext} above $\sim$0.24. As shown in Fig. 3(a), the low-noise GI POFs had lower BERs than the silica GI MMF for all R_{ext} values below and above $\sim$0.24. This result indicates that their lower core refractive indices are not the dominant origin of the BER improvement.

In addition, the net optical feedback level depends on fiber attenuation of A_f. However, for the 1-m evaluated fibers, the influence of the different attenuations on R_{net} is negligible because of their sufficiently low A_f values below 0.014 (0.06 dB). As shown in (2), $\partial R_{net}/\partial A_f < 0$ while $\partial R_{net}/\partial R_{ext} > 0$. Thus, the influence of attenuation change ΔA_f is compensated by a slight change of ΔR_{ext} in R_{ext}. For R_{ext} values below 0.5, the ΔR_{ext} values are on the order of 10^{-3}, being obtained by the condition that $(\partial R_{net}/\partial R_{ext})\Delta R_{ext} + (\partial R_{net}/\partial A_f)\Delta A_f = 0$. As shown in Fig. 3(a), the low-noise GI POFs have lower BERs than the silica GI MMF for the same R_{net} values. Thus, the attenuation difference between the low-noise GI POFs and silica GI MMF only minimally influenced the BER differences.

These analyses show that BER improvement by the low-noise GI POF was likely due to the mode coupling of the low-noise GI POF rather than its lower fiber-facet reflection and higher fiber attenuation than the silica GI MMF. This suggests that any GI POFs with microscopic heterogeneous properties may possess such stabilization effects regardless of the macroscopic material properties of their fiber attenuations and core refractive indices.

To investigate the detailed mechanisms for the BER improvements by the low-noise GI POFs, temporally average noise spectra of the links were measured for various external optical feedback levels. VCSEL instabilities due to external optical feedback have various dynamics depending on the properties of both the VCSEL mode and optical feedback [14], [16], [17]. In the MMF links, problematic optical feedback is due to the partially coherent and partially polarized light backward-guided through the MMFs. Such optical feedback influence on a multimode VCSEL has not been well investigated. The obtained average noise spectra had complex structures, as shown in Fig. 4.

First, all fibers exhibited periodic peaks with an equal spacing corresponding to the round-trip frequencies ($\sim$100 MHz) of the two imaginary external cavities with external reflectors at the HR mirror and at the fiber output face. Therefore, the spikes are external-cavity-mode beatings, indicating that unstable external-cavity-modes were generated owing to external optical feedback from the reflectors. However, the low-noise GI POFs had a much smaller number of peaks and much lower peak levels than did the silica GI MMF, being most pronounced for GI POF Y with its stronger mode coupling. These features are attributed to the stabilization effects of the low-noise GI POF.

For the low-noise GI POF, several envelope peaks were also observed around $\sim$6 GHz, which is the average relaxation frequency of the solitary VCSEL. These envelope peaks may be related to the VCSEL-mode-dependent relaxation frequencies, which are influenced by optical feedback. Numbers of envelope peaks and the dominant peak were intermittently changed, and the average spectra shown in Figs. 4(b) and (c) reflect the most-frequently observed states. As external optical feedback level increased, the separated peaks tended to grow into coupled envelope peaks, and the coupled envelope width tended to broaden for higher feedback levels.

However, the silica GI MMF had completely different spectra from the low-noise GI POFs. As shown in Fig. 4(a), a pronounced envelope peak was observed around $\sim$1.5 GHz for all feedback

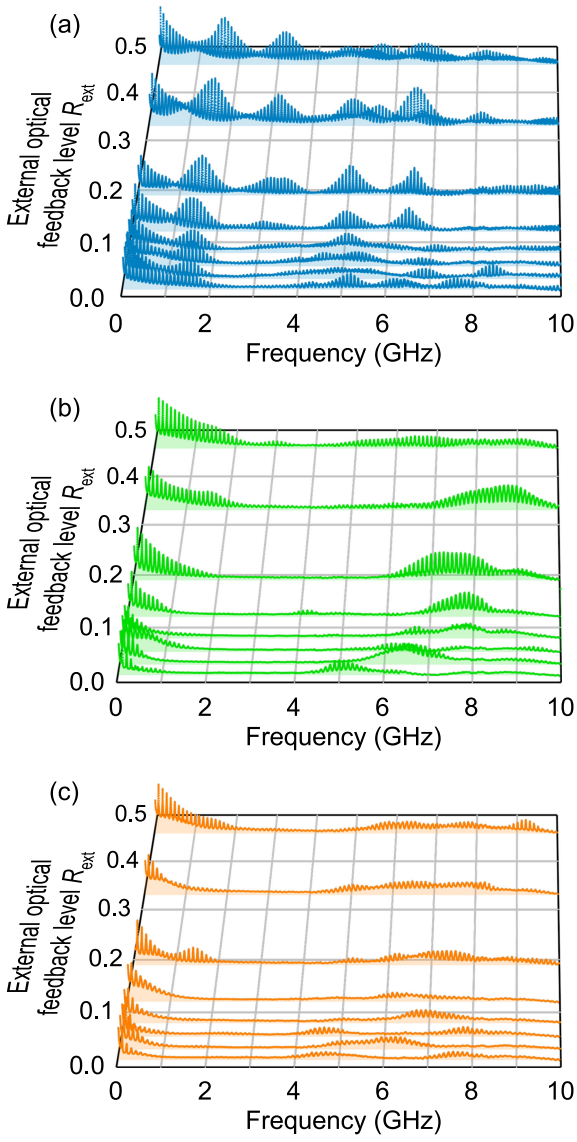

Fig. 4. Average noise spectra change for (a) silica GI MMF, (b) GI POF X, and (c) GI POF Y with an increase in external optical feedback level. The reference plane corresponds to an electrical noise power of −60 dBm. The spectra were obtained by averaging the scanned spectra over 1000 traces with a resolution bandwidth of 10 MHz, a video bandwidth of 30 kHz, and a scan time of 100 ms.

levels. This envelope peak level increased with an increase in external feedback level and transitioned to periodic envelope peaks for optical feedback levels from 0.1 to 0.2. Further feedback-level increases resulted in significant increases in noise floor level through coupling of the envelope peaks accompanying additional peak generation. The spectra with the coupled envelope peaks ranged from dc to ∼10 GHz over the average relaxation frequency of the VCSEL. These spectral transitions and critical destabilizations due to the external optical feedback in the MMF link could be avoided just by using the low-noise GI POF, as shown in Figs. 4(b) and (c). Using GI POF Y with the strongest mode coupling, the critical BER degradation for the external optical feedback levels above ∼0.2 could be avoided [Fig. 3(a)]. To clarify the detailed mechanism for the noise spectral characteristics shown in Fig. 4, it is required to analyze them based on the laser rate equation with consideration of the external optical feedback from the back of the MMF in the MMF link based on a multimode VCSEL.

4. Conclusion

In conclusion, we have demonstrated that a GI POF can significantly stabilize a VCSEL-based MMF link subject to external optical feedback. Our developed GI POF could prevent data transmission quality degradation due to critical destabilization observed in silica GI MMFs. We showed that the dominant mechanism for the stabilization effect is strong mode coupling closely related to microscopic heterogeneities with large-scale density and composition fluctuations, which change the correlation of field patterns, degree of polarization, and degree of coherence of back-reflected lights with the VCSEL modes. This suggests that the stabilization effect may be controlled by the microscopic heterogeneities in the GI POF core materials regardless of the fiber attenuations and core refractive indices. Such a novel concept for link stabilization using the optical fiber itself will facilitate significantly stable data transmission with multilevel modulation in the next-generation of VCSEL-based MMF links for the upcoming IoT era.

Acknowledgment

This paper is based on the results of a project commissioned by the New Energy and Industrial Technology Development Organization (NEDO) of Japan. This study was also supported by the Japan Science and Technology Agency (JST) through the Strategic Promotion of Innovative Research and Development (S-Innovation).

References

[1] N. Bamiedakis *et al.*, "56 Gb/s PAM-4 data transmission over a 1 m long multimode polymer interconnect," presented at the Conf. Lasers Electro-Optics, San Jose, CA, USA, 2015, Paper STu4F.5.
[2] D. Kuchta, "High-capacity VCSEL links," presented at the Optical Fiber Communication Conf., Los Angeles, CA, USA, 2017, Paper Tu3C.4.
[3] Y. Koike, *Fundamentals of Plastic Optical Fibers*. Weinheim, Germany: Wiley-VCH, 2015.
[4] Y. Koike and A. Inoue, "High-speed graded-index plastic optical fibers and their simple interconnects for 4K/8K video transmission," *J. Lightw. Technol.*, vol. 34, no. 6, pp. 1551–1555, Mar. 2016.
[5] A. Inoue and Y. Koike, "Low-noise graded-index plastic optical fiber for significantly stable and robust data transmission," *J. Lightw. Technol.*, vol. 36, no. 24, pp. 5887–5892, Dec. 2018.
[6] J. L. Gimlett and N. K. Cheung, "Effects of phase-to-intensity noise conversion by multiple reflections on gigabit-per-second DFB laser transmission Systems," *J. Lightw. Technol.*, vol. 7, no. 6, pp. 888–895, Jun. 1989.
[7] A. M. J. Koonen, "Bit-error-rate degradation in a multimode fiber optic transmission link due to modal noise," *IEEE J. Sel. Areas Commun.*, vol. SAC-4, no. 9, pp. 1515–1522, Dec. 1986.
[8] B. Hillerich and E. Weidel, "Polarization noise in single mode fibres and its reduction by depolarizers," *Opt. Quantum Electron.*, vol. 15, no. 4, pp. 281–287, 1983.
[9] R. Olshansky, "Propagation in glass optical waveguides," *Rev. Mod. Phys.*, vol. 51, no. 2, pp. 341–367, 1979.
[10] A. Inoue, T. Sassa, K. Makino, A. Kondo, and Y. Koike, "Intrinsic transmission bandwidths of graded-index plastic optical fiber," *Opt. Lett.*, vol. 37, no. 13, pp. 2583–2585, 2012.
[11] A. Inoue *et al.*, "Efficient group delay averaging in graded-index plastic optical fiber with microscopic heterogeneous core," *Opt. Exp.*, vol. 21, no. 14, pp. 17379–17385, 2013.
[12] D. Marcuse, *Theory of Dielectric Optical Waveguides*. New York, NY, USA: Academic, 1974.
[13] K. Petermann, *Laser Diode Modulation and Noise*. Dordrecht, The Netherlands: Kluwer, 1988.
[14] J. Ohtsubo, *Semiconductor Lasers - Stability, Instability and Chaos*. Berlin, Germany: Springer-Verlag, 2013.
[15] M. Salem and G. P. Agrawal, "Coupling of stochastic electromagnetic beams into optical fibers," *Opt. Lett.*, vol. 34, no. 18, pp. 2829–2831, 2009.
[16] J. Y. Law and G. P. Agrawal, "Feedback-induced chaos and intensity-noise enhancement in vertical-cavity surface-emitting lasers," *J. Opt. Soc. Amer. B*, vol. 15, no. 2, pp. 562–569, 1998.
[17] A. Quirce, A. Valle, C. Giménez, and L. Pesquera, "Intensity noise characteristics of multimode VCSELs," *J. Lightw. Technol.*, vol. 29, no. 7, pp. 1039–1045, Apr. 2011.